IET Journals
The Institution of Engineering and Technology

ISSN 1751-8644
doi: 0000000000
www.ietdl.org

Distributed Energy Management for Community Microgrids Considering Phase Balancing and Peak Shaving

Guodong Liu[1]*, Thomas B. Ollis*[1]*, Bailu Xiao*[1]*, Xiaohu Zhang*[2]*, Kevin Tomsovic*[3]

[1] *Oak Ridge National Laboratory, One Bethel Valley Road, P.O. Box 2008, MS 6007, Oak Ridge,37831, USA*
[2] *Global Energy Interconnection Research Institute North America (GEIRINA), 250 W. Tasman Dr., San Jose, 95134, USA*
[3] *Department of Electrical Engineering and Computer Science (EECS), The University of Tennessee, Knoxville, 1520 Middle Dr., Knoxville, 37996, USA*
** E-mail: liug@ornl.gov*

Abstract: In this paper, a distributed energy management for community microgrids considering phase balancing and peak shaving is proposed. In each iteration, the house energy management system (HEMS) installed in each house minimizes its electricity costs and the costs associated with the discomfort of customers due to deviations in indoor temperature from customers' set points. At the community level, the microgrid central controller (MCC) schedules the distributed energy resources (DERs) and energy storage based on the received load profiles from customers and the forecast energy price at the point of common coupling. The MCC updates the energy price for each phase based on the amount of unbalanced power between generation and consumption. The updated energy price and unbalanced power for each phase are distributed to the HEMSs on corresponding phases. When the optimization converges, the unbalanced power of each phase is close to zero. Meanwhile, the schedules of DERs, energy storage systems and the energy consumption of each house, are determined by the MCC and HEMSs, separately. In particular, the phase balancing and peak shaving are considered in the proposed distributed energy management model. The effectiveness of the proposed distributed energy management has been demonstrated by case studies.

Nomenclature

The symbols used in this paper are defined as following. A symbol with (k) at the upper right position stands for its value at the *k*-th iteration. A bold symbol stands for its corresponding vector.

0.1 Indices and Numbers

i	Index of DGs, running from 1 to N_G.
j	Index of loads, running from 1 to N_D.
b	Index of energy storage systems, running from 1 to N_B.
h	Index of houses, running from 1 to H_Φ.
t	Index of time periods, running from 1 to N_T.
ϕ	Index of phases, running from 1 to N_Φ
m	Index of energy blocks offered by DGs, running from 1 to N_I.

0.2 Variables

0.2.1 Binary Variables:

u_{it}	1 if DG i is scheduled on during period t and 0 otherwise.
$u^{\mathrm{C}}_{\phi ht}, u^{\mathrm{H}}_{\phi ht}$	1 if HVAC of house h on phase ϕ is scheduled for cooling/heating during period t and 0 otherwise.
$u^{\mathrm{C}}_{bt}, u^{\mathrm{D}}_{bt}$	1 if energy storage system b is scheduled for charging/discharging during period t and 0 for idling.

0.2.2 Continuous Variables:

$p_{it}\,(m)$	Power output scheduled from the m-th block of energy offer by DG i during period t. Limited to $p^{\max}_{it}\,(m)$.
P_{it}	Power output scheduled from DG i during period t.
$P_{it\phi}$	Power output scheduled from DG i to phase ϕ during period t.
$P^{\mathrm{C}}_{bt}, P^{\mathrm{D}}_{bt}$	Charging/discharging power of energy storage system b during period t.
$P^{\mathrm{C}}_{bt\phi}, P^{\mathrm{D}}_{bt\phi}$	Charging/discharging power of energy storage system b on phase ϕ during period t.
SOC_{bt}	State of charge of energy storage system b during period t.
$P^{\mathrm{PCC}}_{\phi t}$	Scheduled power at PCC on phase ϕ during period t.
$P_{\phi ht}$	Total scheduled load of house h on phase ϕ during period t.
$P^{\mathrm{LS}}_{\phi ht}$	Scheduled voluntary load curtailment of house h on phase ϕ during period t.
$T^{\mathrm{In}}_{\phi ht}$	Indoor temperature of house h on phase ϕ during period t.
$T^{\mathrm{M}}_{\phi ht}$	Temperature of thermally accumulating layer of inner walls and floor in house h on phase ϕ during period t.
$T^{\mathrm{E}}_{\phi ht}$	Temperature of house h envelope on phase ϕ during period t.
$\lambda_{\phi t}$	Lagrange multiplier of power balance equation on phase ϕ during period t.
$R_{\phi t}$	Unbalance between generation and demand of phase ϕ during period t.

0.3 Constants

$\lambda^{P}_{it}\,(m)$	Marginal cost of the m-th block of energy offer by DG i during period t.
$\lambda^{\mathrm{PCC}}_{t}$	Purchasing price of energy from distribution grid during period t.

$P^{\mathrm{PCC,max}}$ Maximum peak load at PCC.
γ_t Maximum phase unbalance at PCC.
ρ Penalty parameter of augmented Lagrangian function.
C_{bt} Degradation cost of energy storage system b during period t.
$V^{\mathrm{LS}}_{\phi ht}$ Cost of voluntary load curtailment of house h on phase ϕ during period t.
$P^{\max}_i, P^{\min}_i$ Maximum/minimum output of DG i.
$P^{\mathrm{W}}_{\phi t}$ Wind turbine power output on phase ϕ during period t.
$P^{\mathrm{PV}}_{\phi t}$ PV power output on phase ϕ during period t.
$P^{\mathrm{O}}_{\phi ht}$ Non-HVAC load of house h on phase ϕ during period t.
$P^{H}_{\phi h}$ Rated power of HVAC system in house h on phase ϕ.
$P^{\mathrm{C,max}}_b, P^{\mathrm{D,max}}_b$ Maximum charging/discharging power of energy storage system b.
$SOC^{\max}_{bt}, SOC^{\min}_{bt}$ Maximum/minimum state of charge of energy storage system b during period t.
$\alpha_{\phi ht}$ Maximum percentage of curtailable load of house h on phase ϕ during period t.
$\eta^{\mathrm{C}}_b, \eta^{D}_b$ Energy storage system charging/discharging efficiency.
$\omega_{\phi ht}$ Discomfort cost of customers of house h during period t.
$\delta_{\phi ht}$ Allowed indoor temperature deviation of house h during period t.
κ_i Operating cost of DG i at the point of $P^{\min}_i$
T^{A}_t Ambient temperature during period t.
$T^{\mathrm{D}}_{\phi ht}$ Desired indoor temperature of house h on phase ϕ during period t.
Ψ_t Solar irradiance during period t.
$\eta_{\phi h}$ Coefficient of performance of HVAC in house h on phase ϕ.
$R^{\max}$ Maximum allowed primal residual for convergence.

1 Introduction

A microgrid can be defined as a low-voltage power system comprising various distributed energy resources (DERs) collocated with loads. It can be operated either grid-connected or islanded from the utility grid [1]. When grid-connected, a microgrid interacts with the utility distribution system through the point of common coupling (PCC). Power could be imported from or exported to the utility system under an agreement. In addition, a microgrid can provide various ancillary services, such as frequency regulation and voltage support in response to the request of the utility [2, 3]. Once the utility distribution network is faulted, a microgrid automatically transforms from grid-connected mode into islanded mode and continues to serve its islanded portion without any interruptions. By integrating renewable generation, energy storage devices, flexible loads, advanced control, and information and communication technology, a microgrid provides a new scheme of electricity supply with high reliability and low costs and emissions [4]. These benefits of microgrids have prompted a growing amount of research from both academia and industry [5].

In general, a microgrid central controller (MCC) performs the energy management of a microgrid in both modes. The MCC determines the output power of controllable distributed generators (DGs), charging/discharging power of energy storage devices, and the imported/exported power from/to the utility system by solving an optimization problem. The optimization problem is usually formulated to minimize the system operating cost while satisfying various constraints related with characteristics of components and/or reliability of the electricity supply [6]. Various models for microgrid energy management in islanded mode [7–9] and grid-connected mode [10–16] have been proposed in the existing literature. In particular, [10–12] proposed deterministic programming models that ignore the uncertainty of renewable generation, while stochastic and robust programming models that consider the uncertainty of renewable generation, have been presented in [13–16].

In general, the vast majority of proposed microgrid energy management systems in the existing literature are based on solving a centralized optimization problem. Although these methods are straightforward and easy to implement, two problems are associated with them. First, energy consumption by consumers is mostly considered as fixed or interruptible loads in the form of direct load control (DLC). However, the customers are usually very careful while allowing a utility or an MCC to directly control their appliances—such as water heaters and heating, ventilation, and air-conditioning (HVAC) systems—because of various issues, such as psychological safety and privacy protection. Second, the centralized optimization model is subject to 'the curse of dimensionality'. As the number of customers increases, the solution efficiency is reduced rapidly. To overcome these issues, distributed optimization models based on dual decomposition are proposed in [17–20]. Since the variables of DERs and each house are only coupled by the power balance constraint, the centralized optimization model can be decoupled into subproblem of DERs and subproblem of each house. The home energy management system (HEMS) in each house solves the corresponding subproblem to determine the schedule of house appliances, while the MCC solves the subproblem of DERs to determine the schedule of DGs and energy storage systems. During each iteration, the Lagrangian multipliers are adjusted based on the imbalance of power supply and consumption. Then, the schedule of DERs and house appliances are updated by the MCC and each HEMS, separately. The iteration repeats until the power supply and consumption are balanced, i.e., the power balance constraint is satisfied. By this method, the MCC no longer needs to control the appliances of customers directly. Similar to dual decomposition, other distributed optimization algorithms, such as the predictor corrector proximal multiplier (PCPM) [21], have been applied to solve the microgrid energy management problem in a distributed manner. To ensure the convergence of the dual decomposition algorithm, convexity and finiteness are assumed for all subproblems. In practice, however, the subproblems are usually nonconvex owing to binary constraints (on/off of generators and HVAC systems), leading to nonconvergence of the optimization.

In this paper, a new distributed energy management for community microgrids is developed. The single-phase model in [22] is extended into a practical three-phase unbalanced model to enable the adjustment of loads and generation in specific phases. The alternating direction method of multipliers (ADMM) algorithm is used to decompose the centralized optimization into parallel subproblems of DERs and HEMSs [23]. The main contributions of this paper in addition to [22] are the following:

- Reducing the phase unbalance of the microgrid at the PCC to avoid mal-operation of zero-sequence protections and potentially provide phase balancing service. In particular, phase-wise price signals are proposed to enable the adjustment of loads and generation in specific phases. Note that the phase balancing function is an innovative contribution of this paper.
- Adding the function of peak shaving for the community microgrid controller to reduce demand charge. This function can also be used for emergency load shedding by setting the PCC power limits in specified intervals to certain percentage of normal PCC power.

For the rest of this paper, the community microgrids and thermal dynamic model of buildings are introduced in Section II. In Section III, centralized optimization-based microgrid energy management is formulated. Based on that, distributed energy management for microgrids is developed in Section IV. The proposed distributed energy management is demonstrated on a community microgrid in Section V. The paper is finally concluded in Section VI.

2 System Model

2.1 Community Microgrid

As an alternative way to increase local energy supply independence and resilience, a community microgrid is a specially kind of microgrid normally serving a residential community. Various DGs and energy storage systems are installed on-site to ensure a continuous and reliable electricity supply to customers even in the face

of widespread blackouts. For each house, a HEMS is installed and schedules all appliances in the house based on user settings, such as desired indoor temperature, and communicates with the MCC for price signals or control orders. In a centralized optimization-based microgrid energy management system, the user settings, consumption schedule of house appliances as well as detailed house thermal dynamic model are all forwarded to the MCC by the HEMSs. Based on this received information, as well as the rate/price from the utility, the MCC determines the optimal schedule of DGs, energy storage, and home appliances by solving a centralized optimization that minimizes the total cost of operating the community microgrid while preserving customer comfort. The optimal schedules of home appliances are sent to the corresponding HEMSs, which will control the HVAC and other appliances accordingly. An example of the community microgrid is shown in Figure 1.

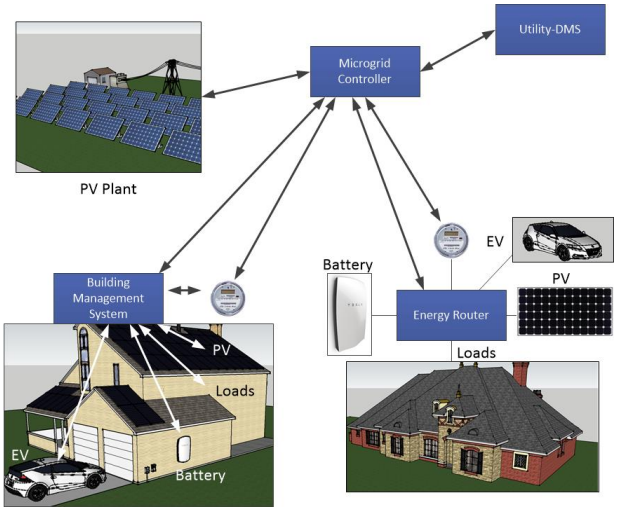

Fig. 1: Example community microgrid

Unlike in centralized optimization-based microgrid energy management, the HEMSs actually withhold user settings, house thermal parameters, and other load information from the MCC in the proposed distributed energy management system. Specifically, the HEMS schedules the appliances in the house based on the price signal received from the MCC to minimize the electricity bill while ensuring user comfort. Meanwhile, the MCC determines the schedule of DERs at the microgrid level to optimize certain objectives. The price signal is iteratively updated based on the power unbalance between generation and load. When this iterative process converges, the HEMSs and MCC reach a consensus on the price signal and energy consumption of each house.

2.2 HVAC System

An HVAC system is usually controlled by a thermostat. In the case of cooling, for instance, the HVAC is switched on when the indoor temperature reaches the upper limit of the allowed indoor temperature range, then continues running until the lower limit is reached. Thermostats based on this automatic temperature control scheme are widely used.

In a departure from the automatic temperature control scheme described, the HEMS intelligently optimizes the consumption of HVAC as well as other house appliances to reduce the electricity cost and discomfort of customers. As is known, the change of indoor temperature is a gradual process because of the thermal inertia of the house. A house could be taken as a thermal storage facility, which provides the HEMS extra flexibility in scheduling the HVAC system. Specifically, the HVAC system can be switched on to pre-cool/preheat the house during times when electricity prices are low or renewable generation is high. Thus the house can ride through peak-price periods without high electricity consumption and still maintain the indoor temperature within an allowable range. This method is expected to achieve significant electricity cost savings compared with autonomous temperature control [15].

2.3 Building Thermal Dynamic Model

Intelligent control of the HVAC system requires to model the house as a thermostatically controlled load (TCL), which is related with a number of factors, including thermal capacitance of indoor air, inner walls and house envelope, thermal resistance between indoor air, inner walls, house envelope, and ambient air, effective window area, etc. There has been extensive research on the accurate modeling of thermal dynamics of houses/buildings. In this work, a two-layer thermal insulation model is utilized to model each house. Based on the rules of heat transfer, the thermal dynamic characteristic of a house could be modeled as first order differential equations in continuous time. Then, these differential equations can be further transformed into equivalent discrete time model by using Euler discretization (i.e., zero-order hold) with a constant sampling time [24]. In this paper, the thermal dynamic model of a house is described by the following state space model.

$$\boldsymbol{T}_{\phi h,t+1} = \boldsymbol{A}_{\phi h}\boldsymbol{T}_{\phi h,t} + \boldsymbol{B}_{\phi h}\boldsymbol{U}_{\phi h,t} \quad \forall\phi,\ \forall h,\ \forall t \tag{1}$$

where $\boldsymbol{T}_{\phi h,t} = \left[T^{\mathrm{In}}_{\phi ht},\ T^{M}_{\phi ht},\ T^{E}_{\phi ht}\right]$ is the state vector, which indicates the temperatures at different layers of the house. $\boldsymbol{U}_{\phi h,t} = \left[T^{A}_{t},\ \Psi_t,\ \left(u^{\mathrm{H}}_{\phi ht} - u^{\mathrm{C}}_{\phi ht}\right)\eta_{\phi h}P^{H}_{\phi h}\right]$ is the input vector, which includes the ambient temperature, solar irradiance and the heat transferred by the HVAC system. In specific, $u^{\mathrm{H}}_{\phi ht} = 1$ corresponds to the heating mode of the HVAC system and $u^{\mathrm{C}}_{\phi ht} = 1$ corresponds to the HVAC cooling mode. The coefficients of matrices $\boldsymbol{A}_{\phi h}$ and $\boldsymbol{B}_{\phi h}$ of a house h on phase ϕ could be determined with the thermal parameters of the house and the time step size of the optimization horizon. More details on the mathematical modeling and parameter estimation of the house can be found in [24]. The indoor temperature for house h is limited in a comfortable range as in (2).

$$T^{D}_{\phi ht} - \delta_{\phi ht} \le T^{\mathrm{In}}_{\phi ht} \le T^{D}_{\phi ht} + \delta_{\phi ht} \tag{2}$$

3 Centralized Community Microgrid Energy Management

In community microgrids, on-site DERs and the utility distribution feeder together supply electricity to all houses. The on-site DERs are divided into two categories: dispatchable units and nondispatchable units. The dispatchable units includes various DGs (e.g., diesel generators, combined heat and power, fuel cells, etc.) and energy storage systems(e.g., batteries and pump-hydro), which could be dispatched by the MCC. On the contrary, renewable generation resources (e.g., photovoltaic systems) are nondispatchable units with power output depending on weather conditions. The community microgrid imports/exports power from/to the utility through the PCC. All DGs, renewable generation resources, and energy storage systems are assumed to be three-phase balanced. Each house is associated with an HVAC load, and the other loads in the house are aggregated as an interruptible load, a certain percentage of which could be shed. All house loads are assumed to be single-phase. All houses are distributed on an average on three phases. Under these assumptions, a centralized optimization problem for the energy management of community microgrids is formulated. The objective is usually to minimize the operation and maintenance cost as well as the discomfort of customers due to indoor temperature deviations, as in equation (3). Specifically, the piecewise linear operation cost and start-up cost of DGs are represented in line 1 and 2; the purchasing/selling cost/benefit of the microgrid at PCC is in line 3; the degradation cost of energy storage systems is in line 4; and finally, the discomfort and inconvenience of customers caused by indoor temperature deviations and voluntary load shedding for each house are described in line 5.

$$\min \quad \sum_{t=1}^{N_T}\sum_{i=1}^{N_G}\left[\sum_{m=1}^{N_I}\lambda_{it}^{P}(m)p_{it}(m)+\kappa_i u_{it}\right]\triangle t + \sum_{t=1}^{N_T}\sum_{i=1}^{N_G} SU_{it}\left(u_{it},u_{i,t-1}\right) + \sum_{t=1}^{N_T}\sum_{\phi=1}^{N_\Phi}\lambda_t^{\mathrm{PCC}}P_{\phi t}^{\mathrm{PCC}}\triangle t + \sum_{t=1}^{N_T}\sum_{b=1}^{N_B}C_{bt}\left(P_{bt}^{\mathrm{C}}+P_{bt}^{\mathrm{D}}\right)\triangle t + \sum_{t=1}^{N_T}\sum_{\phi=1}^{N_\Phi}\sum_{h=1}^{H_\Phi}\left(\omega_{\phi ht}\left|T_{\phi ht}^{\mathrm{In}}-T_{\phi ht}^{D}\right|+V_{\phi ht}^{\mathrm{LS}}P_{\phi ht}^{\mathrm{LS}}\right) \quad (3)$$

The reliable and efficient operation of a community microgrid is subject to various limits and constraints from DERs, customers as well as the MCC.

$$P_{it}=\sum_{m=1}^{N_I}p_{it}(m)+u_{it}P_i^{\min} \quad \forall i,\forall t \quad (4)$$

$$0\le p_{it}(m)\le p_{it}^{\max}(m) \quad \forall i,\forall t,\forall m \quad (5)$$

$$P_i^{\min}u_{it}\le P_{it}\le P_i^{\max}u_{it} \quad \forall i,\forall t \quad (6)$$

$$P_{it\phi}=P_{it}/N_\Phi \quad \forall i,\forall t,\forall\phi \quad (7)$$

$$0\le P_{bt}^{\mathrm{C}}\le P_b^{\mathrm{C,max}}u_{bt}^{\mathrm{C}} \quad \forall b,\forall t \quad (8)$$

$$0\le P_{bt}^{\mathrm{D}}\le P_b^{\mathrm{D,max}}u_{bt}^{\mathrm{D}} \quad \forall b,\forall t \quad (9)$$

$$u_{bt}^{\mathrm{C}}+u_{bt}^{\mathrm{D}}\le 1 \quad \forall b,\forall t \quad (10)$$

$$SOC_{bt}=SOC_{b,t-1}+P_{bt}^{\mathrm{C}}\eta_b^{\mathrm{C}}\triangle t-P_{bt}^{\mathrm{D}}\frac{1}{\eta_b^{\mathrm{D}}}\triangle t \quad \forall b,\forall t \quad (11)$$

$$SOC_{bt}^{\min}\le SOC_{bt}\le SOC_{bt}^{\max} \quad \forall b,\forall t \quad (12)$$

$$P_{bt\phi}^{\mathrm{C}}=P_{bt}^{\mathrm{C}}/N_\Phi \quad \forall b,\forall t,\forall\phi \quad (13)$$

$$P_{bt\phi}^{\mathrm{D}}=P_{bt}^{\mathrm{D}}/N_\Phi \quad \forall b,\forall t,\forall\phi \quad (14)$$

$$P_{\phi ht}=\left(u_{\phi ht}^{\mathrm{H}}+u_{\phi ht}^{\mathrm{C}}\right)P_{\phi h}^{\mathrm{H}}+P_{\phi ht}^{\mathrm{O}} \quad \forall\phi,\forall h,\forall t \quad (15)$$

$$u_{\phi ht}^{\mathrm{H}}+u_{\phi ht}^{\mathrm{C}}\le 1 \quad \forall\phi,\forall h,\forall t \quad (16)$$

$$0\le P_{\phi ht}^{\mathrm{LS}}\le \alpha_{\phi ht}\%P_{\phi ht}^{\mathrm{O}} \quad \forall h,\forall t \quad (17)$$

The power output of a DG is divided into several blocks in equation (4). Each block is limited by a maximum value as in constraint (5). The operating cost in each block is assumed linear. Thus, the operating cost of the DG is piecewise linear. The minimum and maximum power output of DGs are limited by the constraint (6). In particular, DG outputs are three-phase balanced, which is ensured by (7). For energy storage, the charging and discharging power of an energy storage system is constrained by (8) and (9). The charging and discharging states of energy storage are mutually exclusive, a condition enforced by (10). The state of charge (SOC) of an energy storage system at the end of current time period t is determined by the SOC at previous time period $t-1$, plus/minus the energy charged/discharged during current time period. This coupling relationship is described in equation (11). To avoid overcharging and undercharging of an energy storage system, the SOC is limited as in equation (12). The loss during the charging and discharging process is described with the parameters η_b^{C} and η_b^{D}. Similar to DGs, energy storage devices are phase-balanced, which is ensured by the constraints of (13) and (14). For DGs and energy storage systems with unbalanced output, we could simply relax equation (7), (13) and (14) to make sure the sum of generated/consumed power at all phases equals the total power for each DG and energy storage system. For each house, the total load of house h on phase ϕ at time t equals the HVAC load plus the aggregated rest loads, as in constraint (15). The heating and cooling states of a HVAC system are mutually exclusive, as is guaranteed by constraint (16). The voluntary load shedding of house h during time period t is limited by a certain percentage of the aggregated load specified by the customer as shown in constraint (17). Note that the thermal dynamic characteristic of a house (1) and the indoor temperature requirements (2) should be included as constraints as well.

Beside the constraints associated with each component or house, there are several system level constraints, such as generation and load balance, peak load limits, and maximum phase unbalance at the PCC. The generation and load balance on each phase is guaranteed by (18). In particular, wind and PV systems could be balanced three-phase or single-phase sources. The peak load seen by the utility at PCC is limited, as in (19), which could be requested by the utility or required by the MCC to reduce the demand charge. Note that the peak shaving in this paper is realized by real-time pricing (RTP). Other methods, such as demand charge [25], will be investigated in future work. To avoid mal-operation of zero-sequence protections, the maximum phase unbalance at the PCC is constrained by (20). Note that the phase coupling has been ignored for two reasons. First, the feeders in community microgrids are mostly single-phase laterals. Second, these feeders are usually short because of the limited capacity and low voltage level of microgrids.

$$\sum_{i=1}^{N_G}P_{it\phi}+P_{\phi t}^{W}+P_{\phi t}^{\mathrm{PV}}+\sum_{b=1}^{N_B}\left(P_{bt\phi}^{\mathrm{D}}-P_{bt\phi}^{\mathrm{C}}\right)+P_{\phi t}^{\mathrm{PCC}}=\sum_{h=1}^{H_\Phi}\left(P_{\phi ht}-P_{\phi ht}^{\mathrm{LS}}\right) \quad \forall\phi,\forall t \quad (18)$$

$$\sum_{\phi=1}^{N_\Phi}P_{\phi t}^{\mathrm{PCC}}\le P^{\mathrm{PCC,max}} \quad \forall\phi,\forall t \quad (19)$$

$$-\gamma_t\le P_{\phi t}^{\mathrm{PCC}}-P_{\phi' t}^{\mathrm{PCC}}\le\gamma_t \quad \forall\phi,\forall\phi'\ne\phi,\forall t \quad (20)$$

It should be noted that the centralized optimization is a mixed-integer linear programming (MILP) except the two logic terms in the objective function (3), which could be easily formulated in linear or mixed-integer linear (MIL) form by introducing auxiliary variables. In specific, by introducing a binary variable, the start-up cost of DG (in line 2) could be represented in MIL form [26]. As to the absolute value of the indoor temperature deviation (in line 5), it could be substituted by an auxiliary variable $X_{\phi ht}$ with constraints (21) - (23). In general, this centralized optimization problem could be solved by various commercial MILP solvers.

$$X_{\phi ht}\ge T_{\phi ht}^{\mathrm{In}}-T_{\phi ht}^{D} \quad \forall\phi,\forall h,\forall t \quad (21)$$

$$X_{\phi ht}\ge T_{\phi ht}^{D}-T_{\phi ht}^{\mathrm{In}} \quad \forall\phi,\forall h,\forall t \quad (22)$$

$$X_{\phi ht}\ge 0 \quad \forall\phi,\forall h,\forall t \quad (23)$$

More complicated phase-coupled internal models of DGs and energy storage systems need to be considered if their outputs are unbalanced or reactive power is considered. Under this situation, piecewise linearization techniques could be used to formulate these nonlinear models into special-ordered-sets-of-type 2 (SOS2) constraints [27]. As a result, the dimension of the problem, especially the number of binary variables, will increase significantly. Nevertheless, the optimization model is still MILP.

4 Distributed Community Microgrid Energy Management

The centralized community microgrid energy management presented in Section III is straightforward and easy to solve. However, this model is subject to dimensional and privacy issues in practical implementation, since the HVAC systems and voluntary load shedding are directly controlled by the MCC. First of all, the dimension of the optimization problem rises rapidly with the growth of customer scale, which compromises the solution efficiency. As a result, more computing resources are required by the MCC. Besides, the MCC requires access to the thermal dynamic models and detailed load information for all houses, whereas customers generally prefer to conceal all information behind the meters and control their home appliances by themselves. Therefore, our objective is to break down the centralized optimization and obtain a distributed, scalable, privacy-preserving microgrid energy management.

In this section, we propose a distributed algorithm to solve the centralized optimization model (1)-(23) using ADMM [23]. The centralized optimization model has a separable structure, since the only constraint (18) is a complicating constraint involving variables from both the microgrid level and the house level. Therefore, we use ADMM to decompose the centralized optimization model into optimization subproblems at the microgrid and house levels. The subproblems are solved by the MCC and the HEMSs separately, and the solutions are coordinated by an iterative process.

$$\begin{aligned} R_{\phi t}^{(k)} &= \sum_{i=1}^{N_G} P_{it\phi}^{(k)} + P_{\phi t}^{W} + P_{\phi t}^{\mathrm{PV}} + \sum_{b=1}^{N_B} \left(P_{bt\phi}^{\mathrm{D,(k)}} - P_{bt\phi}^{\mathrm{C,(k)}} \right) \\ &\quad + P_{\phi t}^{\mathrm{PCC,(k)}} - \sum_{h=1}^{H_\Phi} \left(P_{\phi ht}^{(k)} - P_{\phi ht}^{\mathrm{LS,(k)}} \right) \ \forall \phi, \forall t \end{aligned} \tag{24}$$

Initially set at $k \leftarrow 0$, the HEMSs schedule their appliances randomly and communicate them to the MCC. In the meantime, the MCC sets initial price curves for each phase and schedules the microgrid-level resources randomly. At the beginning of each iteration, the MCC updates the unbalanced power of each phase according to (24) and communicates the prime residual $R_{\phi t}^{(k)}$ and price signal $\lambda_{\phi t}^{(k)}$ to the corresponding HEMSs connected to each phase. Then the following process occurs.

1. Each HEMS solves the HEMS subproblem as follows:

$$\begin{aligned} \min \quad & \sum_{t=1}^{N_T} \left(\omega_{\phi ht} \left| T_{\phi ht}^{\mathrm{In}} - T_{\phi ht}^{D} \right| + V_{\phi ht}^{\mathrm{LS}} P_{\phi ht}^{\mathrm{LS}} \right) \\ & - \sum_{t=1}^{N_T} \lambda_{\phi t}^{(k)} \left[R_{\phi t}^{(k)} + \left(P_{\phi ht}^{(k)} - P_{\phi ht}^{\mathrm{LS},(k)} \right) \right. \\ & \left. - \left(P_{\phi ht} - P_{\phi ht}^{\mathrm{LS}} \right) \right] \\ & + \frac{\rho}{2} \left\| \mathbf{R}_{\phi}^{(k)} + \left(\mathbf{P}_{\phi h}^{(k)} - \mathbf{P}_{\phi h}^{\mathrm{LS},(k)} \right) \right. \\ & \left. - \left(\mathbf{P}_{\phi h} - \mathbf{P}_{\phi h}^{\mathrm{LS}} \right) \right\|_2^2 \end{aligned} \tag{25}$$

s.t.

$$(1),\ (2)\,,\ (15)-(17), \text{and}\ (21)-(23)$$

2. The MCC solves the MCC subproblem as follows:

$$\begin{aligned} \min \quad & \sum_{t=1}^{N_T} \sum_{i=1}^{N_G} \left[\sum_{m=1}^{N_I} \lambda_{it}^{P}(m) p_{it}(m) + \kappa_i u_{it} \right] \triangle t \\ & + \sum_{t=1}^{N_T} \sum_{i=1}^{N_G} SU_{it} + \sum_{t=1}^{N_T} \sum_{\phi=1}^{N_\Phi} \lambda_t^{\mathrm{PCC}} P_{\phi t}^{\mathrm{PCC}} \triangle t \\ & + \sum_{t=1}^{N_T} \sum_{b=1}^{N_B} C_{bt} \left(P_{bt}^{\mathrm{C}} + P_{bt}^{\mathrm{D}} \right) \triangle t \\ & - \sum_{t=1}^{N_T} \sum_{\phi=1}^{N_\Phi} \lambda_{\phi t}^{(k)} \left[R_{\phi t}^{(k)} - \sum_{i=1}^{N_G} P_{it\phi}^{(k)} - P_{\phi t}^{\mathrm{PCC,(k)}} \right. \\ & - \sum_{b=1}^{N_B} \left(P_{bt\phi}^{\mathrm{D,(k)}} - P_{bt\phi}^{\mathrm{C,(k)}} \right) + \sum_{i=1}^{N_G} P_{it\phi} \\ & \left. + P_{\phi t}^{\mathrm{PCC}} + \sum_{b=1}^{N_B} \left(P_{bt\phi}^{\mathrm{D}} - P_{bt\phi}^{\mathrm{C}} \right) \right] \\ & + \frac{\rho}{2} \sum_{\phi=1}^{N_\Phi} \left\| \mathbf{R}_{\phi}^{(k)} - \sum_{i=1}^{N_G} \mathbf{P}_{i\phi}^{(k)} - \mathbf{P}_{\phi}^{\mathrm{PCC,(k)}} \right. \\ & - \sum_{b=1}^{N_B} \left(\mathbf{P}_{b\phi}^{\mathrm{D,(k)}} - \mathbf{P}_{b\phi}^{\mathrm{C,(k)}} \right) + \sum_{i=1}^{N_G} \mathbf{P}_{i\phi} \\ & \left. + \mathbf{P}_{\phi}^{\mathrm{PCC}} + \sum_{b=1}^{N_B} \left(\mathbf{P}_{b\phi}^{\mathrm{D}} - \mathbf{P}_{b\phi}^{\mathrm{C}} \right) \right\|_2^2 \end{aligned} \tag{26}$$

s.t.

$$(4)-(14)\,,\ \text{and}\ (19)-(20)$$

At the end of each iteration, the HEMSs communicate their updated schedules $P_{\phi ht}^{(k)}$ and $P_{\phi ht}^{\mathrm{LS},(k)}$ to the MCC, then the MCC updates the prime residual $R_{\phi t}^{(k+1)}$ and price signal $\lambda_{\phi t}^{(k+1)}$ according to (24) and (27). This iterative process is repeated until convergence occurs. In this distributed optimization scheme, prices are iteratively negotiated between customers and generators (including DGs, energy storage and utility). Therefore, this approach has the advantage of being self-contained in the sense that it does not need other price constraints, because price procurement is based on an iterative negotiation process.

$$\lambda_{\phi t}^{(k+1)} = \lambda_{\phi t}^{(k)} - \rho R_{\phi t}^{(k+1)} \tag{27}$$

A complete description of the proposed distributed energy management system can be found in Algorithm 1. Compared with traditional dual decomposition algorithm, ADMM adds an augmented Lagrangian term with a penalty factor $\rho > 0$. This augmented Lagrangian term is introduced in part to bring robustness to the dual decomposition algorithm, and particularly to yield convergence when assumptions of strict convexity and finiteness of (3) are no longer valid. In other words, ADMM improves the classic dual decomposition algorithm with the superior convergence properties of augmented Lagrangian methods. Note that ADMM cannot guarantee a global optimum like other nonconvex optimization algorithms. The convergence of ADMM for nonconvex problem has not been proved mathematically. In practice, the solution might oscillate around an optimum because of the nonconvexity of the integer variables. In this situation, a suboptimal solution can still be obtained for practical use by increasing the penalty factor ρ or relaxing the converge criterion $R^{\max}$. Nevertheless, it is often the case that ADMM converges to modest accuracy within a few tens of iterations [23].

Algorithm 1 Proposed Distributed Community Microgrid Energy Management

1: **initialization** $k \leftarrow 0$. The HEMSs set their initial schedules randomly, or using forecasted/historical load, and send them to the MCC. The MCC sets the initial price randomly, or using historical prices, and schedules the microgrid-level resources.
2: **repeat**
3: The MCC updates the primal residual of each phase $R_{\phi t}^{(k)}$ and sends the two signals $R_{\phi t}^{(k)}$ and $\lambda_{\phi t}^{(k)}$ to the corresponding HEMSs connected to each phase;
4: The HEMS of each house updates its schedule by solving the HEMS subproblem;
5: The MCC updates the schedule of microgrid-level resources by solving the MCC subproblem;
6: The HEMSs send the updated total consumption and load shedding back to the MCC, then the MCC updates $R_{\phi t}^{(k+1)}$ and updates $\lambda_{\phi t}^{(k+1)}$;
7: $k \leftarrow k+1$;
8: **until** $(R_{\phi t}^{(k+1)} \leq R^{\max})$

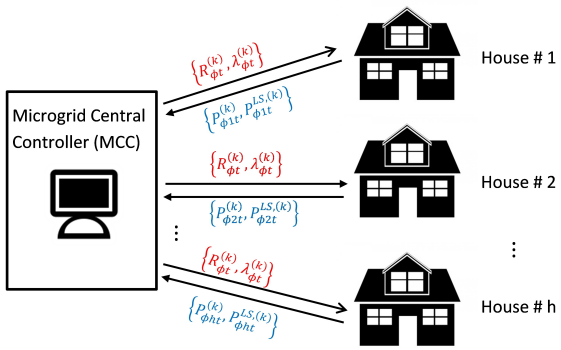

Fig. 2: Exchange of Information between MCC and HEMSs

In this distributed energy management system, the power unbalance and price signals of each phase are broadcasted to the corresponding HEMSs through the advanced metering infrastructures (AMIs). For each house, the HEMS subproblem (25) is solved, then the total consumption $P_{\phi ht}^{(k)}$ and voluntary load shedding $P_{\phi ht}^{\mathrm{LS},(k)}$ are communicated to the MCC. In this way, customers have absolute control over their HVAC systems and other appliances behind the meter. In addition, the schedules of individual appliances and customer preferences are concealed from the MCC. Therefore, the privacy of customers is preserved. Fig. 2 illustrates the information exchange between the MCC and HEMSs.

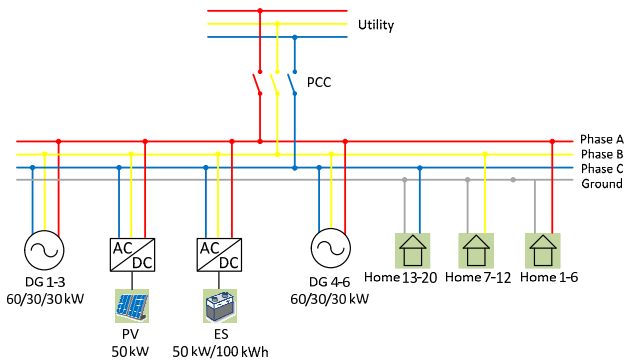

Fig. 3: Community microgrid test system

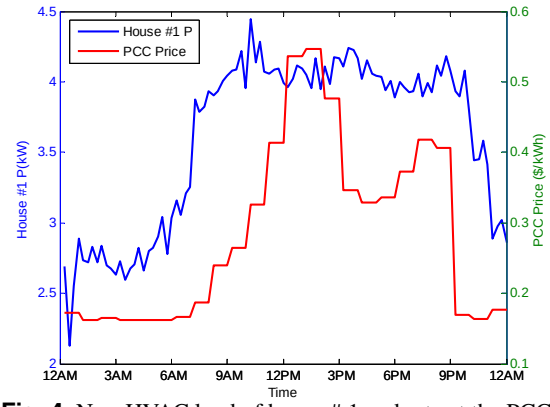

Fig. 4: Non-HVAC load of house # 1 and rate at the PCC

Table 1 Parameters of MPC

Time Resolution	Prediction Horizon	Control Horizon	Recalculation Time
15 min	24 hour	1 hour	1 hour

5 Case Studies

The proposed distributed energy management was tested using a Oak Ridge National Laboratory (ORNL) microgrid test system as shown in Fig. 3. All DGs, PVs, and batteries are assumed to have three-phase balanced output/input. Their parameters can be found in [16]. The community microgrid supplies electricity to 20 houses. A 5kW HVAC system is installed in each house. The coefficients of performance (COP) of all HVAC systems are set as $\eta_h = 3$. For simplicity, the desired room temperatures of all houses during the whole scheduling horizon are set at 23°C. To avoid excessively rapid cycling of the HVAC systems, the indoor temperature is allowed to deviate ±2 °C from the set point. The temperature deviations lead to discomfort of customers, which is penalized at \$0.05/°C. The maximum voluntary load shedding is limited as 50% of the non-HVAC load in each house, with the price of lost load set as the PCC price doubled. The thermal dynamic models of the houses are taken from [24] (Table 7.1 in [24]). Small random errors are introduced to represent the diversity of houses. The ambient temperature and solar irradiance are the measured data of the Oak Ridge, Tennessee, area on 1 August, 2015 [28], which is a typical summer day in the southern states of the US.

The forecast non-HVAC load of house # 1 and the electricity price at the PCC are shown in Fig. 4. All houses are assumed to have the same non-HVAC loads. The penalty parameter ρ is set as 0.1. The initial price is set as 0.1 \$/kWh for all time intervals. The simulation is conducted of a day (24 hours) with 15-min time resolution. Noted that the forecasts of load and renewable resources are subject to errors, which usually increase rapidly as the forecast horizon increases. To handle the uncertainty of forecasts, model predictive control (MPC) has been used in power system balancing models considering uncertain forecasts [29]. For example, if the load and renewable forecasts are updated every hour, the optimization should be run every hour, but only schedules of the first hour will be implemented into the system and the rest will be discarded. The parameters of MPC in this case are summarized in Table 1. In this work, the forecast errors for load and renewable resources have been neglected in the simulation since the MPC approach doesn't change the proposed optimization model and solution algorithm, but repeatedly run the optimization with the most recent forecast data.

All problems are solved using the commercial MILP solver CPLEX 12.6. With a pre-specified duality gap of 0.5%, the solution time of centralized optimization is about 15 minutes on a 2.66 GHz Windows-based PC with 4 GB of RAM. For the distributed optimization, the solution time of each subproblem is less than 10 seconds using the same computer. Since all subproblems are solved

Table 2 Total operating cost of the community microgrid in different cases

Cases	Autonomous Thermostat Control ($)	Base Case ($)	Base Case + Phase Balancing ($)	Base Case + Peak Shaving ($)	Base Case + Phase Balancing + Peak Shaving ($)
Centralized Optimization	397.95	294.04	294.15	294.26	294.38
Distributed Optimization		294.08	294.40	294.89	295.20
Difference (%)	N/A	0.01	0.08	0.21	0.28

in parallel, the total solution time distributed optimization is around 3 minutes.

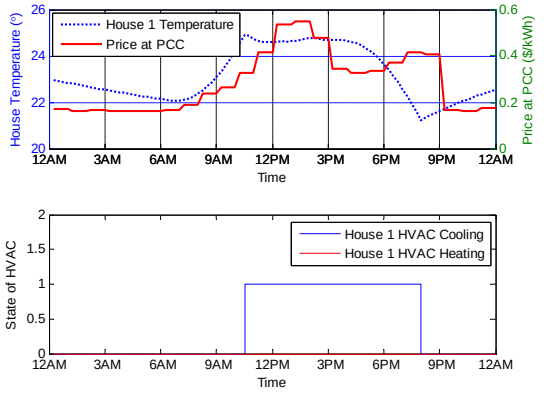

(a) Autonomous Thermostats Control

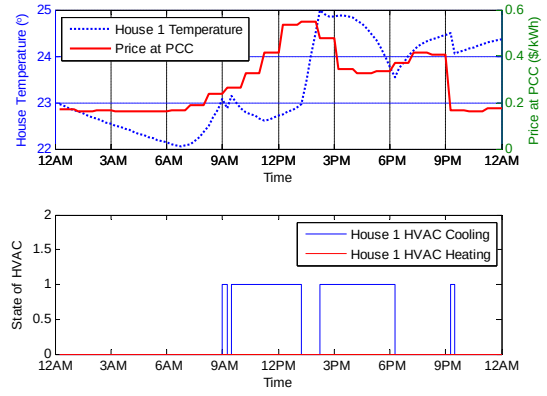

(b) Base Case: Centralized Optimization

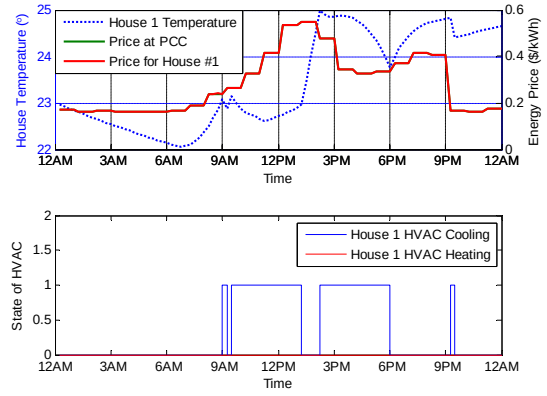

(c) Base Case: Distributed Optimization

Fig. 5: House #1 indoor temperature and HVAC status in autonomous thermostat control and the base case

5.1 *Comparing Costs of Different Cases*

The total operating costs of the community microgrid in various cases are compared in this section. The test cases include autonomous thermostatic control (without considering building thermal dynamics in the optimization), base case (considering building thermal dynamics in the optimization), base case with phase balancing constraints, base case with peak shaving constraints, and finally, base case with both phase balancing and peak shaving constraints. In the case of autonomous thermostat control, equation (1) is solved first, then the thermostats determine the on/off state of the HVAC system based on the internal temperature controlled relay circuit. Given the HVAC states, we solve the centralized optimization and obtain the total operating cost as in (3).

The costs are compared in Table 2. First, compared with autonomous thermostat control, the total operating cost of the base case is reduced by 26.11% by integrating building thermal dynamics in the optimization. The cost savings is significant for community microgrids, in which HVAC systems dominate the load. Second, compared with the base case, adding the phase balancing and/or peak shaving constraints to the base case has very little effect on the total operating cost. Note that the base case could be considered as our previous work in [22]. In other words, the functions of phase balancing and peak shaving are realized in this paper with very little additional cost compared to [22]. This also indicates that HVAC energy consumption can easily be shifted for phase balancing and peak shaving without obvious effects on system operating cost and customer discomfort. Third, as mentioned earlier, ADMM converges to a local optimum. However, comparing the difference between the costs of centralized optimization and of distributed optimization, the proposed distributed algorithm has almost the same performance as centralized optimization; i.e., the solution is very close to the global optimum.

The calculated indoor temperature and HVAC status of house #1, in the cases of autonomous thermostat control and the base case are compared in Fig. 5. Comparing Fig. 5a with Fig. 5b and 5c, it clearly shows, in the base case (considering building thermal dynamics in the optimization), the HVAC cooling is switched on around 9 A.M. when the indoor temperature is perfectly 23°C., i.e., the set point. Thus, the house is precooled during low price periods to avoid or reduce the consumption of HVAC during peak price periods (1 P.M. – 2 P.M. and 7 P.M. – 8 P.M.), so that the electricity bill of the customer is reduced. Since the PCC can be seen as the marginal unit in this case, the price for house #1 converges to the PCC price, as shown in Fig. 5c.

5.2 *Distributed Energy Management with Constraints of Phase Balancing or/and Peak Shaving*

The maximum phase unbalance and total power at the PCC in the different cases solved by the proposed distributed energy management method are compared in Fig. 6. For the phase balancing constraint, the maximum difference in power between any two phases for all time intervals is limited to less than 20 kW. For the peak shaving constraint, the peak demand at the PCC is limited to less than 50 kW. As can be seen in Fig. 6a, the maximum phase unbalance is reduced to less than 20 kW for the cases with the phase balancing constraint. Similarly, the total power at the PCC is reduced to be less than 50 kW for the cases with peak shaving constraint, as can be seen in Fig. 6b. When both constraints are considered, the maximum phase unbalance and total power at the PCC are reduced to the corresponding limits simultaneously. It should be noted that

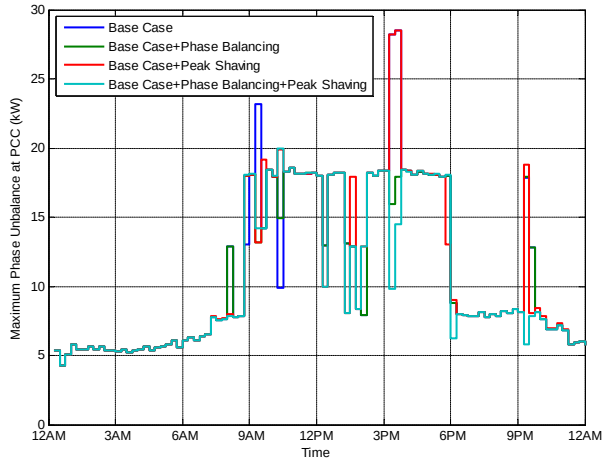

(a) Maximum phase unbalance

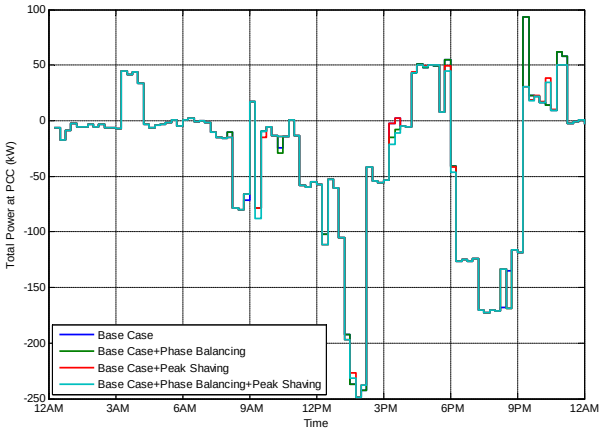

(b) Total power at PCC

Fig. 6: Maximum phase unbalance and total power at PCC solved by proposed distributed optimization for different cases

unwanted demand spikes occur during the periods of 3 A.M. – 4 A.M. and 10 P.M. – 11 P.M. The reason is that the energy price at the PCC is very low during these hours, which causes the shutdown of all DGs.

It should be noted that the peak shaving function can also be used for emergency load shedding. For example, if the community microgrid is requested by the utility to reduce its imported power at PCC by 50% in the next 15 minutes. The MCC can simply reset the PCC power limit in the next time interval to 50% of the power imported in normal situation.

5.3 Convergence of the Proposed Distributed Energy Management

For the case with both phase balancing and peal shaving constraints, the converged price signals for all three phases and the utility rate at the PCC are compared in Fig. 7. As can be seen, the price curves for all three phases generally follow the utility rate at the PCC except for three periods (9 A.M. – 10 A.M., 3 P.M. – 4 P.M. and 9 P.M. – 10 P.M.). In the periods 9 A.M. – 10 A.M. and 3 P.M. – 4 P.M., the prices in phase C are extremely high. This is because the load in phase C is much higher than in phases A and B (see Fig. 6a). Thus, high price signals are generated to reduce the energy consumption of houses connected to phase C during these periods. Like congestion pricing in transmission level wholesale market, the synchronized consumption on phase C causes an unbalanced issue in this case. As a result,

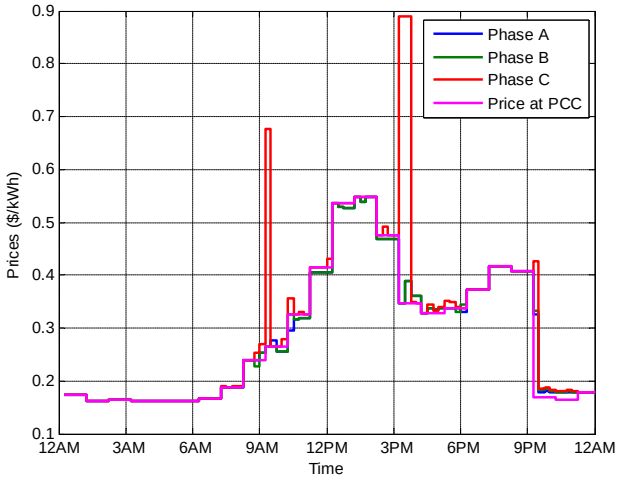

Fig. 7: Converged price signal $\lambda_{\phi t}$ in the case with both phase balancing and peak shaving constraints

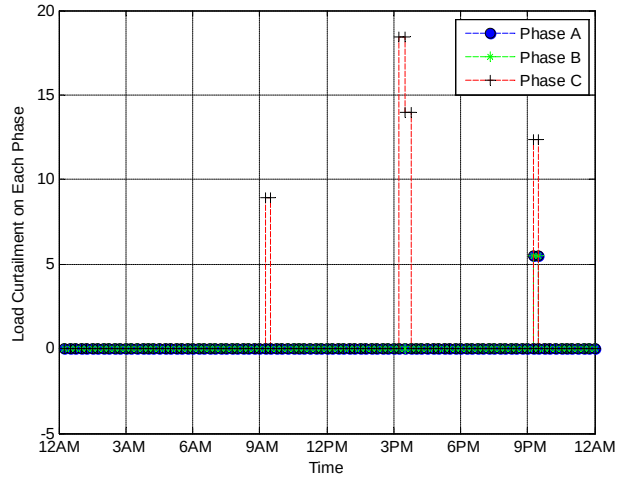

Fig. 8: Load curtailment in the case with both phase balancing and peak shaving constraints

a penalty price is generated to solve this issue. Similarly, during the period 9 P.M. – 10 P.M., the price signals for all three phases are higher than the utility rate at the PCC. This is because the total load at the PCC exceeds the peak demand limits (see Fig. 6b). As a result, high price signals are generated to reduce the energy consumption of houses on all three phases during this period.

For the case with both phase balancing and peak shaving constraints, the load curtailments on all three phases over the scheduling horizon are shown in Fig. 8. As can be seen, during the periods of 9 A.M. - 10 A.M. and 3 P.M. - 4 P.M., only loads on phase C are curtailed for phase balancing. However, during the period 9 P.M. - 10 P.M., the loads on all three phases are curtailed for peak shaving.

Although there are several convergence criterions for the ADMM algorithm (e.g., prime residual convergence, objective convergence and dual variable convergence), a reasonable convergence criterion for the proposed distributed energy management for community microgrids is that the primal residual $R_{\phi t}$ must be very small, i.e., the total generation equals the total consumption for each phase. The satisfaction of this criterion means the MCC and customers (both DERs and consumers) reach an agreement on the price and the amount of electricity generation/consumption. The primal residual could be calculated according to equation (24), and the stopping criterion used in the simulation is $R_{\phi t} \leq 0.5$. The primal residual

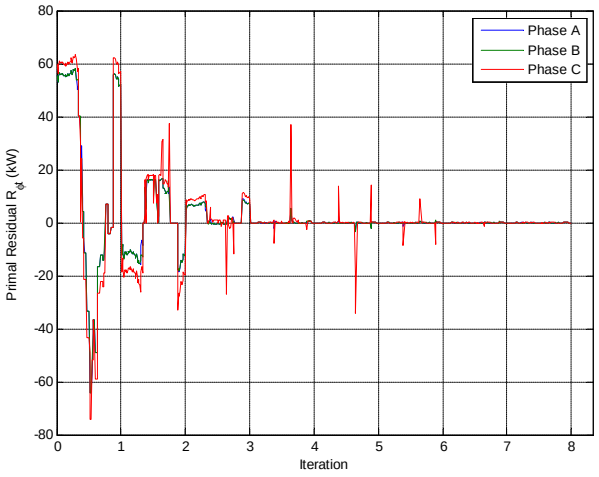

Fig. 9: Primal residual versus iteration

of three phases as a function of the iteration number is shown in Fig. 9. For each iteration, the primal residuals of all time intervals are included and shown in chronological order. As can be seen, the proposed distributed optimization converges after eight iterations. ADMM can be very slow to converge at high accuracy. However, it usually can produce acceptable results for practical use within a few tens of iterations.

6 Conclusions

In this paper, a distributed energy management model for community microgrids considering phase balancing and peak shaving is proposed. Given the price signals and unbalance power between generation and demand received from the MCC, the HEMS in each house optimizes its electricity cost and the customer's comfort, considering the thermal dynamic model of the house. Then, the MCC optimizes the output of DERs and energy storage at the microgrid level, updates the price signals and unbalance power, and then communicates them to the houses connected to the corresponding phases. In particular, the phase balancing and peak shaving constraints are considered in the proposed model. In the proposed distributed energy management, the MCC guides the consumption of customers with price signals instead of direct load control. The distributed energy management model is solved by an ADMM algorithm. The effectiveness of the proposed model is demonstrated by the results of numerical simulations.

7 Acknowledgments

This work is supported by the U.S. Department of Energy's Office of Electricity Delivery and Energy Reliability (OE) under Contract No. DE-AC05-00OR22725. This work also made use of Engineering Research Center Shared Facilities supported by the Engineering Research Center Program of the National Science Foundation and the Department of Energy under NSF Award Number EEC-1041877 and the CURENT Industry Partnership Program.

8 References

1 'The CERTS Microgrid Concept', https://certs.lbl.gov/sites/all/files/lbnl-50829.pdf, October 2003
2 Madureira A.G., Pecas Lopes, J.A.: 'Coordinated voltage support in distribution networks with distributed generation and microgrids', *IET Renew. Power Gen.*, 2009, **3**, (4), pp. 439-454
3 Beer, S., Gomez, T., Dallinger, D., *et al.*: 'An economic analysis of used electric vehicle batteries integrated into commercial building microgrids', *IEEE Trans. Smart Grid*, 2012, **3**, (1), pp. 517-525
4 Tsikalakis, A.G., Hatziargyriou, N.D.:'Centralized control for optimizing microgrids operation', *IEEE Trans. Energy Convers.*, 2008, **23**, (1), pp. 241-248
5 Agrawal, M., Mittal, A.: 'Microgrid technological activities across the globe: A review', *Int. J. Res. Rev. Appl. Sci.*, 2011, **7**, (2), pp. 147-152
6 Gu, W., Wu, Z., Bo, R., *et al.*: 'Modeling, planning and optimal energy management of combined cooling, heating and power microgrid: A review', *Int. J. Electr. Power Energy Syst.*, 2014, **54**, pp. 26-37
7 Chen, F., Chen, M., Li, Q., *et al.*: 'Cost-Based Droop Schemes for Economic Dispatch in Islanded Microgrids', *IEEE Trans. Smart Grid*, 2017, **8**, (1), pp. 63-74
8 Olivares, D.E., Canizares, C.A., Kazerani, A.: 'A Centralized Energy Management System for Isolated Microgrids', *IEEE Trans. Smart Grid*, 2014, **5**, (4), pp. 1864-1875
9 Oh, S., Chae, S., Neely, J., *et al.*: 'Efficient Model Predictive Control Strategies for Resource Management in an Islanded Microgrid', *Energies*, 2017, **10**, (7), 1008
10 Bracco, S., Brignone, M., Delfino, F., *et al.*: 'An Energy Management System for the Savona Campus Smart Polygeneration Microgrid', *IEEE Syst. J.*, 2017, **11**, (3), pp. 1799-1809
11 Li, Z., Xu, Y.: 'Optimal coordinated energy dispatch of a multi-energy microgrid in grid-connected and islanded modes', *Applied Energy*, 2018, **210**, pp. 974-986
12 Martinez Cesena, E.A., Good, N., Syrri, A., *et al.*: 'Techno-economic and business case assessment of multi-energy microgrids with co-optimization of energy, reserve and reliability services', *Applied Energy*, 2018, **210**, pp. 896-913
13 Sheikhahmadi, P., Mafakheri, R., Bahramara, S., *et al.*: 'Risk-Based Two-Stage Stochastic Optimization Problem of Micro-Grid Operation with Renewables and Incentive-Based Demand Response Programs', *Energies*, 2018, **11**, (3), 610
14 Su, W., Wang, J., Roh, J.: 'Stochastic Energy Scheduling in Microgrids With Intermittent Renewable Energy Resources', *IEEE Trans. Smart Grid*, 2014, **5**, (4), pp. 1876-1883 2014.
15 Nguyen, D.T., Le, L.B.: 'Optimal Bidding Strategy for Microgrids Considering Renewable Energy and Building Thermal Dynamics', *IEEE Trans. Smart Grid*, 2014, **5**, (4), pp. 1608-1620
16 Liu, G., Xu, Y., Tomsovic, K.: 'Bidding Strategy for Microgrid in Day-Ahead Market Based on Hybrid Stochastic/Robust Optimization', *IEEE Trans. Smart Grid*, 2016, **7**, (1), pp. 227-237
17 Gatsis, N., Giannakis, G.B.: 'Residential load control: Distributed scheduling and convergence with lost AMI messages', *IEEE Trans. Smart Grid*, 2012, **3**, (2), pp. 770-786
18 Moradzadeh, B., Tomsovic, K.: 'Two-Stage Residential Energy Management Considering Network Operational Constraints', *IEEE Trans. Smart Grid*, 2013, **4**, (4), pp. 2339-2346
19 Liu, T., Tan, X., Sun, B., *et al.*: 'Energy management of cooperative microgrids: A distributed optimization approach', *Int. J. Electr. Power Energy Syst.*, 2018, **96**, pp. 335-346
20 Zhang, Y., Gatsis, N., Giannakis, G.: 'Robust energy management for microgrids with high-penetration renewables', *IEEE Trans. Sustain. Energy*, 2013, **4**, (4), pp. 944-953
21 Shi, W., Xie, X., Chu C., *et al.*: 'Distributed Optimal Energy Management in Microgrids', *IEEE Trans. Smart Grid*, 2015, **6**, (3), pp. 1137-1146
22 Liu, G., Starke, M., Xiao, B., *et al.*: 'A New Distributed Optimization for Community Microgrids Scheduling'. Proc. 50th Hawaii Int. Conf. on Syst. Sci. (HICSS-50),Waikoloa, HI, January 2017, pp. 3045-3054.
23 Boyd, S., Parikh, N., Chu, E., *et al.*: 'Distributed Optimization and Statistical Learning via the Alternating Direction Method of Multipliers', *Foundations and Trends in Machine Learning*, 2011, **3**, pp. 1-122
24 Thavlov, A,: 'Dynamic optimization of power consumption', M.S. thesis, Tech. Univ. Denmark, Kongens Lyngby, Denmark, 2008, pp. 1-120
25 Zhang, Y., Hajiesmaili, M. H., Cai, S., *et al.*: 'Peak-Aware Online Economic Dispatching for Microgrids', *IEEE Trans. Smart Grid*, 2018, **9**, (1), pp. 323-335
26 Carrion, M., Arroyo, J.M. :'A computationally efficient mixed-integer linear formulation for the thermal unit commitment problem', *IEEE Trans. Power Syst.*, 2006, **21**, (3), pp. 1371-1378
27 Guret, C., Prins, C., Sevaux, M. :'Applications of Optimization With Xpress-MP', *Dash Optim. Ltd.*, Blisworth, U.K., 2000
28 'Oak Ridge National Laboratory (ORNL) Rotating Shadowband Radiometer (RSR)', https://www.nrel.gov/midc/ornl_rsr/, accessed, 7 October 2017
29 Wang, Z., Wang, J., Chen, B., *et al.*: 'MPC-Based Voltage/Var Optimization for Distribution Circuits With Distributed Generators and Exponential Load Models', *IEEE Trans. Smart Grid*, 2014, **5**, (5), pp. 2412-2420